Dicle Tıp Dergisi / Dicle Med J (2026) 53 (3) : 701-713

www.diclemedj.org

Original Article / Özgün Araştırma

Protective Effects of Esculetin at two Different Doses on Oxidative Stress, Inflammation, and Fibrotic Changes in $AlCl_3$-Induced Cardiotoxicity in Rats

Tansu Kuşat[1], Feyza Başak[1], Orhan Önalan[2], Ali Şenol[3]

1 Karabuk University, Faculty of Medicine, Department of Histology and Embryology, Karabuk, Türkiye

2 Karabuk University, Faculty of Medicine, Department of Cardiology, Karabuk, Türkiye

3 Kırıkkale University, Faculty of Veterinary Medicine, Department of Biochemistry, Kırıkkale, Türkiye

Received: 27.04.2026; Revised: 28.07.2026; Accepted: 25.08.2026

Abstract

Objective: Aluminum chloride ($AlCl_3$) is an environmental toxicant that promotes cardiotoxicity primarily by inducing oxidative stress and inflammatory responses. Esculetin (ESC), which is a naturally occurring coumarin derivative, possesses antioxidant, anti-inflammatory, and antifibrotic activities. This study evaluated the protective effects of ESC against $AlCl_3$-induced cardiotoxicity, with a focus on dose-related responses.

Methods: 35 male Wistar albino rats were randomly assigned to five experimental groups (n=7 per group): Control, Vehicle, $AlCl_3$ (10 mg/kg), $AlCl_3$ + ESC50 (50 mg/kg), and $AlCl_3$ + ESC100 (100 mg/kg). All experimental treatments were administered orally once daily throughout the 14-day study period. Cardiac tissue levels of malondialdehyde (MDA), reduced glutathione (GSH), superoxide dismutase (SOD), and catalase (CAT) were determined to assess oxidative stress. Tumor necrosis factor-alpha (TNF-α) and interleukin-1 beta (IL-1β) were measured to evaluate the inflammatory response. Histopathological changes and the immunoreactivity of inducible nitric oxide synthase (iNOS) and alpha-smooth muscle actin (α-SMA) were also evaluated.

Results: $AlCl_3$ exposure led to increased MDA levels and decreased GSH levels, with reduced SOD and CAT activities in heart tissue ($P<0.01$). ESC treatment significantly reversed these alterations in both dose groups ($P<0.01$). Furthermore, TNF-α and IL-1β levels were significantly reduced in the ESC-treated groups compared with the $AlCl_3$ group ($P<0.01$). Histopathological examination revealed less myocardial damage in the ESC-treated groups, whereas immunohistochemical analysis showed reduced iNOS and α-SMA immunoreactivity. The protective effects were greater in the 100 mg/kg ESC-treated group.

Conclusion: ESC mitigates $AlCl_3$-induced cardiotoxicity through modulation of oxidative stress and inflammatory responses, improvement of histological findings, and influence on profibrotic alterations. Protective effects were observed with both ESC doses, with generally greater improvements in the higher-dose group.

Keywords: Aluminum chloride, esculetin, cardiotoxicity, inflammation, oxidative stress

DOI: 10.5798/dicletip.2037192

Correspondence / Yazışma Adresi: *Tansu Kusat, Karabuk University, Faculty of Medicine, Department of Histology and Embryology, Karabuk, Türkiye*
e-mail: tansukusat@karabuk.edu.tr

Ratlarda $AlCl_3$ ile İndüklenen Kardiyotoksisitede İki Farklı Dozda Uygulanan Eskuletinin Oksidatif Stres, İnflamasyon ve Fibrotik Değişiklikler Üzerindeki Koruyucu Etkileri

Öz

Amaç: Alüminyum klorür ($AlCl_3$), başlıca oksidatif stres ve inflamasyon aracılığıyla kardiyotoksisiteye neden olan çevresel bir toksik ajandır. Doğal bir kumarin türevi olan eskületin (ESC), antioksidan, antiinflamatuar ve antifibrotik özellikler göstermektedir. Bu çalışmada, ESC'nin $AlCl_3$ ile indüklenen kardiyotoksisite üzerindeki koruyucu etkileri, dozla ilişkili yanıtlar açısından değerlendirilmiştir.

Yöntemler: 35 adet erkek Wistar albino sıçan beş gruba ayrıldı (n=7): kontrol, vehicle, $AlCl_3$ (10 mg/kg), $AlCl_3$ + ESC50 (50 mg/kg) ve $AlCl_3$ + ESC100 (100 mg/kg). Tüm uygulamalar 14 gün boyunca günde bir kez oral yolla gerçekleştirildi. Kalp dokusunda malondialdehit (MDA), indirgenmiş glutatyon (GSH), süperoksit dismutaz (SOD) ve katalaz (CAT) düzeyleri oksidatif stres belirteçleri olarak; tümör nekroz faktör-alfa (TNF-α) ve interlökin-1 beta (IL-1β) düzeyleri ise inflamatuar parametreler olarak değerlendirildi. Ayrıca histopatolojik değişiklikler ile indüklenebilir nitrik oksit sentaz (iNOS) ve alfa-düz kas aktini (α-SMA) immünoreaktivitesi incelendi.

Bulgular: $AlCl_3$ uygulaması kalp dokusunda MDA düzeylerini artırırken, GSH düzeyleri ile SOD ve CAT aktivitelerini azalttı ($P<0.01$). ESC tedavisi her iki doz grubunda bu değişiklikleri anlamlı düzeyde tersine çevirdi ($P<0.01$). Ayrıca, ESC uygulanan gruplarda TNF-α ve IL-1β düzeyleri $AlCl_3$ grubuna kıyasla daha düşük bulundu ($P<0.01$). Histopatolojik incelemede ESC gruplarında miyokardiyal hasarın azaldığı gözlenirken, immünohistokimyasal analizde iNOS ve α-SMA immünoreaktivitesinde azalma saptandı. Koruyucu etkilerin 100 mg/kg ESC uygulanan grupta daha belirgin olduğu dikkati çekti.

Sonuç: ESC, oksidatif stres ve inflamatuvar yanıtları modüle ederek, histopatolojik bulguları iyileştirerek ve profibrotik değişiklikler üzerinde etkili olarak $AlCl_3$ kaynaklı kardiyotoksisiteyi hafifletmektedir. Her iki ESC dozu da koruyucu etkiler göstermiş olup, yüksek doz grubunda genel olarak daha fazla iyileşme saptanmıştır.

Anahtar kelimeler: Alüminyum klorür, esculetin, inflamasyon, kardiyotoksisite, oksidatif stres.

INTRODUCTION

Nowadays, exposure to environmental contaminants is recognized as an increasingly important global public health concern. Aluminum (Al) is a heavy metal frequently encountered in industrial and natural settings[1]. Exposure to Al can arise via consumption of cereals, dairy products, vegetables, and tea, as well as from antacids, phosphate binders, various pharmaceuticals, cosmetics, filtered drinking water, and food additives[2]. Al can enter the body via oral, intranasal, transdermal, and parenteral routes, subsequently accumulating in tissues such as the heart, liver, kidneys, and brain, where it exerts toxic effects[3,4].

Aluminum chloride ($AlCl_3$) is a widely used form of Al in various applications[5]. At the cellular level, $AlCl_3$ disrupts ion balance and interacts with metal-binding proteins, leading to impaired intracellular metal homeostasis, a key mechanism underlying its toxicity[6]. This disturbance promotes excessive production of reactive oxygen species (ROS), disrupting redox homeostasis and leading to oxidative stress. Elevated ROS levels promote lipid peroxidation, thereby compromising cell membrane integrity[1,2,7]. Oxidative stress further stimulates inflammatory signaling cascades, resulting in increased expression of proinflammatory cytokines, including TNF-α and IL-1β[4]. These processes also alter biomarkers associated with inflammation and tissue remodeling in the cardiovascular system. Notably, inducible nitric oxide synthase (iNOS), an enzyme that mediates excessive nitric oxide production during inflammatory responses, as well as alpha-smooth muscle actin (α-SMA), a well-established marker of fibrosis, have been shown to increase in various cardiac pathologies and are therefore commonly utilized as biomarkers in the assessment of heart tissue damage[8,9]. In accordance with these mechanisms,

experimental studies have demonstrated that $AlCl_3$ administration induces pronounced cardiotoxicity by promoting inflammation, necrosis, and fibrotic alterations in cardiac tissue[5]. Moreover, $AlCl_3$ exposure has been reported to elevate malondialdehyde (MDA) levels while suppressing antioxidant defense mechanisms, including glutathione (GSH), superoxide dismutase (SOD), and catalase (CAT)[10].

Cardiotoxicity is recognized as an important clinical consequence of exposure to a variety of toxic agents and contributes substantially to increased morbidity and mortality[11]. The limitations of current therapeutic approaches in mitigating $AlCl_3$-induced cardiotoxicity highlight the need for more effective and reliable alternative strategies, particularly those targeting key pathophysiological mechanisms such as oxidative stress and inflammation[4].

Coumarins are a class of phytochemicals with diverse pharmacological properties. Esculetin (ESC; a coumarin derivative naturally occurring in plants) has attracted considerable interest due to its antioxidant, anti-inflammatory, antifibrotic, and ROS-scavenging activities[12,13]. Evidence suggests that ESC attenuates oxidative stress and reinforces antioxidant defense mechanisms, particularly through the restoration of GSH levels in experimental hepatic and renal toxicity models[14]. Although research on the impact of ESC on the cardiovascular system remains limited, available evidence indicates that ESC exerts protective effects on cardiac tissue through its antioxidant and anti-inflammatory activities. Indeed, ESC is known to exert cardioprotective effects through attenuation of oxidative stress and reduction of cellular damage in experimental cardiotoxicity models[13,15].

Accordingly, the present study was designed to investigate the protective effects of different ESC doses against $AlCl_3$-induced cardiotoxicity by evaluating oxidative stress, inflammatory responses, fibrotic changes, and histopathological alterations.

METHODS

Animal Supply and Experimental Design

Thirty-five male Wistar albino rats (200–250 g) were included and obtained from the Experimental Medicine and Application Unit of Karabük University. The rats were kept in standard cages under controlled environmental conditions (12-h light/dark cycle, 21 ± 1 °C, 50–60% humidity) with free access to food and water.

Animals were randomly allocated to five experimental groups (n = 7 per group). The sample size was determined based on previous experimental studies using similar experimental designs and was considered appropriate according to institutional laboratory practice and ethical considerations. The designated treatments were administered orally once daily throughout the 14-day study period:

1. Control Group: Control group rats received isotonic saline (1 mL).

2. Vehicle Group: Vehicle group rats received 10% dimethyl sulfoxide (DMSO) (1 mL).

3. Aluminum Chloride Group ($AlCl_3$): Rats in the $AlCl_3$ group received aluminum chloride (10 mg/kg), dissolved in isotonic saline[16].

4. $AlCl_3$ + Esculetin 50 mg/kg Group ($AlCl_3$ + ESC50): Rats in this group received aluminum chloride (10 mg/kg). In addition, esculetin (50 mg/kg), dissolved in 10% DMSO, was administered 1 hour after $AlCl_3$ administration[13].

5. $AlCl_3$ + Esculetin 100 mg/kg Group ($AlCl_3$ + ESC100): Rats in this group received aluminum chloride (10 mg/kg). Additionally, esculetin (100 mg/kg), dissolved in 10% DMSO, was administered 1 hour later[13].

Collecting Tissue Samples

At the completion of the experimental protocol, rats were euthanized under ketamine (80 mg/kg) and xylazine (8 mg/kg) anesthesia. Excised heart tissues were gently rinsed with physiological saline to eliminate residual blood prior to further processing. A portion of each heart sample was fixed in 10% neutral buffered formalin for histopathological evaluation, whereas the remaining tissue was preserved at −80 °C for subsequent biochemical analyses.

Biochemical Analysis

Heart tissues were homogenized in phosphate buffer using an IKA Ultra Turrax T25 basic homogenizer at 12,000 rpm for 1–2 min under cold conditions to obtain a 10% (w/v) tissue homogenate. MDA levels were assessed by the thiobarbituric acid reaction, forming a pink chromogen measured at 535 nm. N-butanol and tetramethoxypropane were used as the blank and standard, respectively. The findings were presented as nmol/g wet tissue. Following homogenization, samples were subjected to centrifugation at 4000 rpm for 20 minutes at +4 °C, and the resulting supernatant was then collected for subsequent analyses.

GSH levels were determined using 5,5′-dithiobis (2-nitrobenzoic acid) at 412 nm and reported as nmol/g wet tissue. SOD activity was evaluated based on its ability to inhibit nitroblue tetrazolium reduction through the xanthine–xanthine oxidase system, with absorbance recorded at 560 nm and values reported as U/g protein. CAT activity was evaluated based on hydrogen peroxide (H_2O_2) decomposition at 240 nm over 1 minute and presented as K/g protein. All assays were conducted according to previously described protocols[17]. TNF-α (Catalog No: E0764Ra) and IL-1β (Catalog No: E0119Ra) levels were analyzed using ELISA kits.

Histopathological Analysis

Heart tissues were fixed in 10% neutral buffered formalin for 48 hours, followed by washing under running tap water and subsequent dehydration in graded ethanol series (50–100%), clearing in xylene, and subsequent embedding in paraffin. Serial sections of 5 µm thickness were obtained from paraffin blocks. Sections were stained with hematoxylin and eosin (H&E) for general histological assessment, whereas Masson's trichrome staining was used to evaluate collagen deposition and fibrosis. All sections were examined using a light microscope (Leica DM2500 LED, Leica Microsystems, Germany) equipped with the LAS analysis system. Histopathological damage was assessed in 10 randomly selected microscopic fields per section, focusing on myofibrillar degeneration and disorganization, interstitial inflammatory cell infiltration, and vascular congestion/hemorrhage. Each parameter was graded as 0 (absent), 1 (mild), 2 (moderate), or 3 (severe), yielding a maximum histopathological damage score (MHDS) of 9. In addition to total MHDS values, individual histopathological parameters were also analyzed separately. All histopathological evaluations were performed by an investigator blinded to the experimental groups.

Immunohistochemical Staining

Immunohistochemical staining was carried out using the streptavidin–biotin–peroxidase complex (sABC) method to assess iNOS and α-SMA immunoreactivity. Paraffin sections were deparaffinized with xylene, rehydrated through graded ethanol solutions (100–70%), and subjected to heat-induced antigen retrieval in citrate buffer (pH 6.0) using a microwave oven (600 W) for approximately 15 min. Endogenous peroxidase activity was blocked by incubation with 0.3% H_2O_2 for 20 min, after which tissue

sections were treated with a protein blocking solution for 5 min. The sections were subsequently incubated with primary antibodies against iNOS (Santa Cruz, sc-7271, 1:100) and α-SMA (Santa Cruz, sc-53015, 1:100), followed by secondary antibody and streptavidin-HRP incubation for 30 min each. Diaminobenzidine was used as the chromogen to visualize immunoreactivity, after which the sections were counterstained with Mayer's hematoxylin, dehydrated, cleared, and mounted.

Immunostaining intensity was assessed semi-quantitatively using the H-score system. For each section, ten randomly selected microscopic fields were analyzed at ×20 magnification. Staining intensity was categorized as 0 (none), 1 (weak), 2 (moderate), or 3 (strong). The H-score was calculated as: H-score = Σ Pi (i + 1), where Pi represents the percentage of cells stained at each intensity level (0–100%) 8. Immunohistochemical scoring was also performed under blinded conditions.

Statistical Analysis

Statistical analyses were performed using IBM SPSS Statistics version 25.0 (IBM Corp., Chicago, IL, USA), while graphical figures were prepared with GraphPad Prism version 8 (GraphPad Software, San Diego, CA, USA). Data are presented as mean ± standard deviation (SD). The normality of data distribution was assessed using the Kolmogorov–Smirnov test ($P > 0.05$). For histopathological and immunohistochemical analyses, each animal was considered an independent experimental unit, and statistical comparisons were performed using individual animal scores. Intergroup comparisons were performed using one-way ANOVA followed by Tukey's HSD post hoc test. Statistical significance was defined as $P < 0.01$.

RESULTS

Biochemical Results

Oxidative and antioxidative markers in heart tissue

To evaluate oxidative stress in cardiac tissue, MDA and GSH concentrations together with CAT and SOD activities were determined. Compared with the Control and Vehicle groups, the $AlCl_3$ group exhibited significantly higher MDA levels, along with lower GSH levels and reduced CAT and SOD activities ($P<0.01$, Figure 1). Relative to the $AlCl_3$ group, both ESC-treated groups ($AlCl_3$ + ESC50 and $AlCl_3$ + ESC100) showed significantly higher GSH levels and CAT and SOD activities, whereas MDA levels were significantly lower ($P<0.01$, Figure 1). Furthermore, the $AlCl_3$ + ESC100 group exhibited significantly lower MDA levels and significantly higher GSH levels, as well as increased CAT and SOD activities, compared to the $AlCl_3$ + ESC50 group ($P<0.01$, Figure 1). No significant differences were observed between the Control and Vehicle groups with respect to MDA and GSH levels or CAT and SOD activities ($P>0.05$, Figure 1).

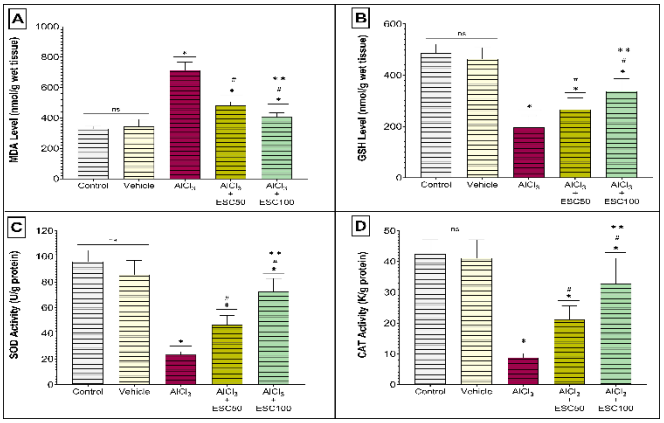

Figure 1. Results for MDA (A), and GSH (B) levels with SOD (C), and CAT (D) activities in heart tissue. Data are expressed as the mean ± SD (n = 7). * indicates a statistically significant difference compared to the Control and Vehicle groups ($P<0.01$); # indicates a statistically significant difference compared to the $AlCl_3$ group ($P<0.01$); ** indicates a statistically significant difference compared to the $AlCl_3$ + ESC50 group ($P<0.01$); ns indicates a statistically nonsignificant

difference compared to the Control and Vehicle groups (P>0.05).

Pro-inflammatory cytokines in heart tissue

Pro-inflammatory cytokines, including TNF-α and IL-1β, were measured in heart tissue. Compared with the Control and Vehicle groups, the $AlCl_3$ group exhibited significantly higher TNF-α and IL-1β levels (P<0.01, Figure 2). In comparison with the $AlCl_3$ group, both ESC-treated groups ($AlCl_3$ + ESC50 and $AlCl_3$ + ESC100) showed significantly lower TNF-α and IL-1β levels (P<0.01, Figure 2). Moreover, the $AlCl_3$ + ESC100 group exhibited significantly lower TNF-α and IL-1β levels than the $AlCl_3$ + ESC50 group (P<0.01, Figure 2). No significant differences in TNF-α or IL-1β levels were detected between the Control and Vehicle groups (P>0.05, Figure 2).

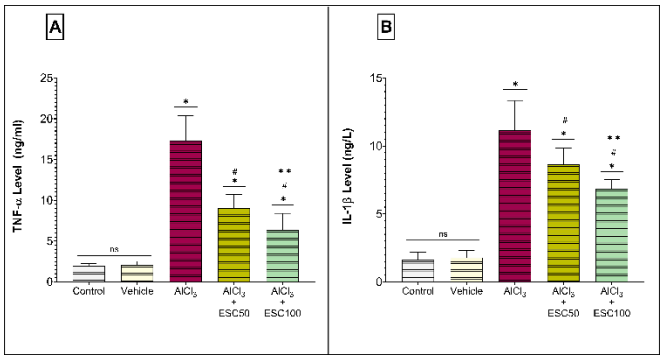

Figure 2. Results of TNF-α (A) and IL-1β (B) levels. Data are expressed as the mean ± SD (n = 7). * indicates a statistically significant difference compared to the Control and Vehicle groups (P<0.01); # indicates a statistically significant difference compared to the $AlCl_3$ group (P<0.01); ** indicates a statistically significant difference compared to the $AlCl_3$ + ESC50 group (P<0.01); ns indicates a statistically nonsignificant difference compared to the Control and Vehicle groups (P>0.05).

Histopathological Alterations in Heart Tissue

Hematoxylin–eosin (H&E) and Masson's trichrome staining

Examination of H&E-stained heart sections by light microscopy revealed preserved myocardial histological architecture in both the Control and Vehicle groups. In these groups, cardiomyocytes were regularly organized, myofibril architecture was maintained, and interstitial spaces appeared normal. Moreover, no notable infiltration of inflammatory cells or vascular congestion was detected in these groups (Figure 3). Conversely, marked histopathological alterations were noted in the $AlCl_3$ group. This group had pronounced myofibril degradation and disarray, notable interstitial inflammatory cell infiltration, accompanied by vascular congestion and regions of bleeding. Furthermore, there was an expansion of interstitial gaps and a significant disturbance of normal myocardial architecture (Figure 3). In the $AlCl_3$ + ESC50 group, histological damage was partially mitigated; inflammatory cell infiltration decreased, vascular congestion was reduced, and myofibril organization showed relative improvement. In the $AlCl_3$ + ESC100 group, the cardiac architecture was predominantly maintained, inflammatory infiltration was diminished, and histological alterations were markedly reduced. The results indicate protective effects of ESC in both treatment groups, with generally greater histopathological improvement observed in the $AlCl_3$ + ESC100 group (Figure 3). The assessment of Masson's trichrome-stained sections demonstrated a normal distribution of collagen fibers in the Control and Vehicle groups. Compared with these groups, the $AlCl_3$ group showed increased perivascular collagen deposition. However, these alterations remained relatively limited at the light microscopic level. In the ESC-treated groups ($AlCl_3$ + ESC50 and $AlCl_3$ + ESC100), collagen deposition appeared less evident than in the $AlCl_3$ group, particularly in the $AlCl_3$ + ESC100 group (Figure 3).

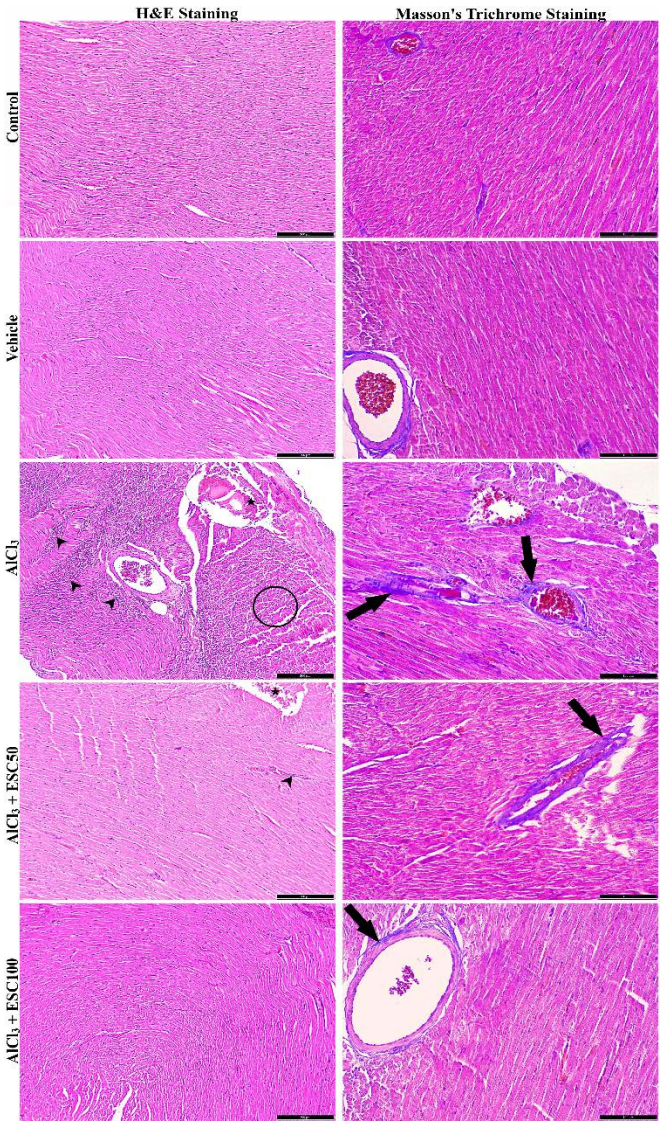

Figure 3. Photomicrographs of heart tissue stained with H&E (scale bar: 200 µm) and Masson trichrome (scale bar: 100 µm). In the $AlCl_3$ group, perivascular collagen deposition was observed together with histopathological alterations, including vascular congestion, inflammatory cell infiltration, and myofibrillar disorganization. These alterations were attenuated in the ESC-treated groups, particularly in the $AlCl_3$ + ESC100 group, in which cardiac tissue architecture was largely preserved. Asterisk: vascular congestion; arrowhead: infiltration of inflammatory cells; circle: disruption of myofibrils; arrow: deposition of collagen.

Table 1 presents the individual histopathological parameters and total MHDS values. Compared with the Control and Vehicle groups, the $AlCl_3$ group exhibited significantly higher scores for myofibrillar degeneration/disorganization, inflammatory cell infiltration, vascular congestion/hemorrhage, and total MHDS ($P<0.01$). Treatment with ESC significantly reduced inflammatory cell infiltration, vascular congestion/hemorrhage, and total MHDS values in both the $AlCl_3$ + ESC50 and $AlCl_3$ + ESC100 groups compared with the $AlCl_3$ group ($P<0.01$). In contrast, a significant reduction in myofibrillar degeneration/disorganization was observed only in the $AlCl_3$ + ESC100 group ($P<0.01$). Furthermore, total MHDS values were significantly lower in the $AlCl_3$ + ESC100 group than in the $AlCl_3$ + ESC50 group ($P<0.01$), whereas inflammatory cell infiltration and vascular congestion/hemorrhage scores did not differ significantly between the two ESC-treated groups ($P>0.05$).

Table 1. Individual histopathological parameters and total histopathological damage score (MHDS) in all experimental groups. Data are expressed as the arithmetic mean ± SD (n = 7). MHDS: mean histopathological damage score. * indicates a statistically significant difference compared to the Control and Vehicle groups ($P<0.01$); # indicates a statistically significant difference compared to the $AlCl_3$ group ($P<0.01$); ** indicates a statistically significant difference compared to the $AlCl_3$ + ESC50 group ($P<0.01$).

GROUP	Myofibrillar Degeneration/ Disorganization	Inflammatory Cell Infiltration	Vascular Congestion/ Hemorrhage	Total MHDS
Control	0.25±0.10	0.28±0.11	0.25±0.09	0.78±0.17
Vehicle	0.30±0.12	0.31±0.10	0.32±0.11	0.93±0.14
$AlCl_3$	2.70±0.20*	2.75±0.18*	2.70±0.25*	8.15±0.83*
$AlCl_3$+ESC50	2.40±0.25*	1.36±0.20$^{*,\#}$	1.34±0.22$^{*,\#}$	5.13±0.42$^{*,\#}$
$AlCl_3$+ESC100	1.10±0.18$^{*,\#,**}$	1.15±0.15$^{*,\#}$	1.14±0.20$^{*,\#}$	3.39±0.78$^{*,\#,**}$

Immunohistochemical detection of iNOS and α-SMA

Immunohistochemical analysis revealed weak iNOS and α-SMA immunoreactivity in the cardiac tissues of both the Control and Vehicle groups (Figure 4). Consistent with these findings, H-score values did not differ significantly between the two groups ($P>0.05$, Figure 5). In contrast, the $AlCl_3$ group showed a marked increase in both iNOS and α-SMA immunoreactivity. Diffuse cytoplasmic iNOS immunostaining was observed predominantly in cardiomyocytes, whereas intense α-SMA immunoreactivity was mainly localized to vascular smooth muscle cells and perivascular areas (Figure 4). Accordingly, H-score values in the $AlCl_3$ group were significantly higher than those recorded in all other experimental groups ($P<0.01$, Figure 5). Compared with the $AlCl_3$ group, the $AlCl_3$ + ESC50 group exhibited mild-to-moderate iNOS and α-SMA immunostaining together with significantly lower H-score values ($P<0.01$, Figure 5). The $AlCl_3$ + ESC100 group showed markedly reduced iNOS and α-SMA immunoreactivity (Figure 4), with H-score values significantly lower than those of both the $AlCl_3$ and $AlCl_3$ + ESC50 groups ($P<0.01$, Figure 5). Overall, these findings indicate that ESC reduced iNOS and α-SMA expression in both treatment groups, with greater reductions observed in the $AlCl_3$ + ESC100 group.

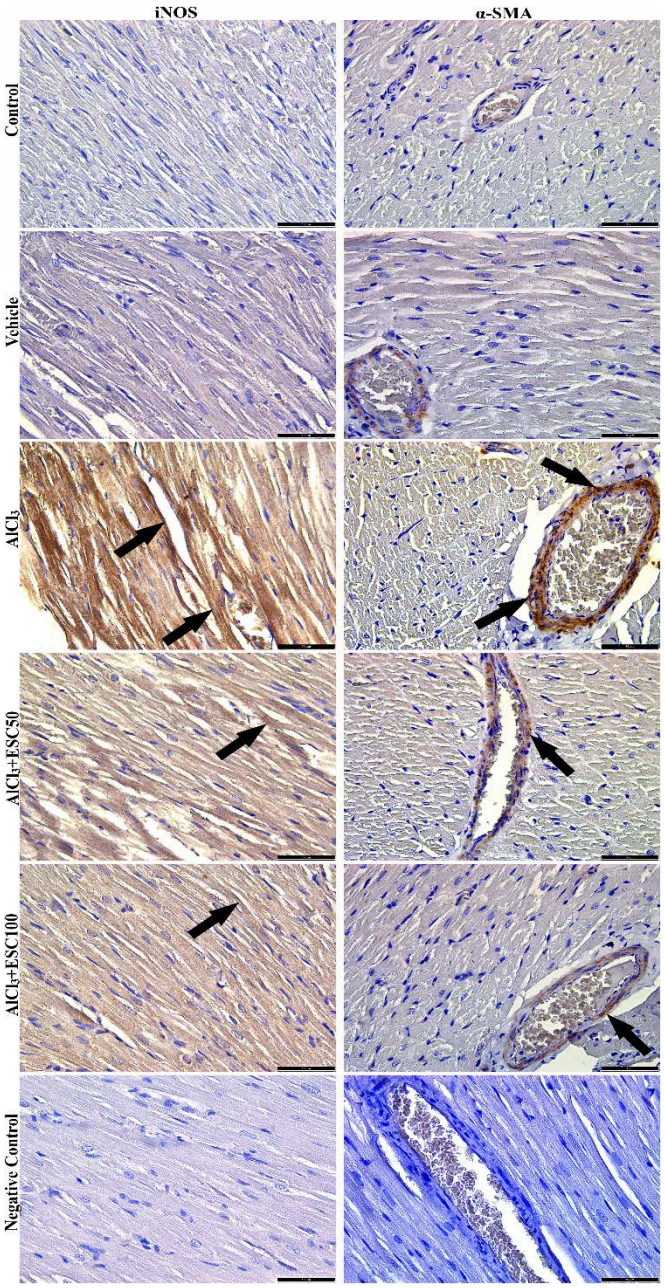

Figure 4. Images of iNOS and α-SMA immunostaining in heart tissue. Arrows indicate positive immunoreactivity. Scale bar: 50 µm.

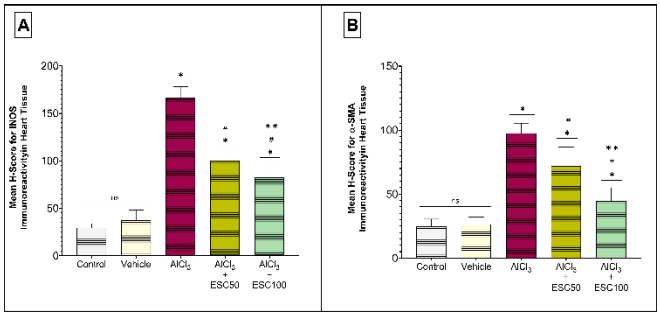

Figure 5. The H-Scores of iNOS (A) and α-SMA (B) immunoreactivity. Data are expressed as the arithmetic mean ± SD (n = 7). * indicates a statistically significant difference compared to the Control and Vehicle groups (P<0.01); # indicates a statistically significant difference compared to the $AlCl_3$ group (P<0.01); ** indicates a statistically significant difference compared to the $AlCl_3$ + ESC50 group (P<0.01); ns indicates a statistically nonsignificant difference compared to the Control and Vehicle groups (P>0.05).

DISCUSSION

Currently, exposure to toxic metals is widely recognized as a major environmental risk factor associated with damage to multiple organ systems[18]. Among these toxic metals, Al is one of the most abundant naturally occurring elements and is extensively distributed throughout the environment[19]. Moreover, human exposure to Al is common because it is present in numerous everyday products, including food, toothpaste, cosmetics, food additives, and pharmaceutical formulations[18], with $AlCl_3$ being widely utilized in experimental models[20]. Dietary surveys conducted in different populations have reported that the average daily intake of Al in adults ranges from 3 to 12 mg, suggesting that routine human exposure is largely unavoidable[21].

Following exposure, $AlCl_3$ tends to accumulate in tissues, leading to toxic effects in multiple organs, most notably the liver, kidneys, heart, and brain, and contributing to the development of hepatotoxicity, nephrotoxicity, and neurodegenerative processes. Furthermore, the toxic effects of $AlCl_3$ on the cardiovascular system have attracted increasing attention in recent years. Epidemiological evidence indicates a significant association between occupational and environmental aluminum exposure and the incidence of cardiovascular diseases, highlighting the susceptibility of the cardiovascular system to Al toxicity[22]. Consistent with these findings, experimental evidence indicates that $AlCl_3$ induces significant cardiotoxic effects in heart tissue[7].

Accordingly, the present study investigated the potential protective effects of ESC against $AlCl_3$-induced cardiotoxicity by evaluating oxidative stress, inflammation, fibrotic changes, and histopathological alterations.

Oxidative stress develops when the generation of reactive oxygen species (ROS) exceeds the capacity of endogenous antioxidant defense systems[18]. One of the mechanisms involved in $AlCl_3$-induced toxicity is the disruption of the oxidant–antioxidant balance due to excessive ROS generation, thereby suppressing key antioxidant defenses, including SOD, GSH, and CAT, and promoting lipid peroxidation, as evidenced by elevated MDA levels[20]. Consistent with these mechanistic observations, experimental studies have demonstrated that $AlCl_3$ exposure induces oxidative stress, characterized by increased MDA levels, decreased GSH levels, and reduced SOD and CAT activities[23]. Indeed, a study examining the protective effect of selenium against $AlCl_3$-induced cardiotoxicity concluded that rats administered $AlCl_3$ for 21 days exhibited a significant increase in MDA levels and a notable suppression of the antioxidant defense system 1. Similarly, in the model of neuroinflammation and cardiometabolic disorder induced by $AlCl_3$ and sodium azide, increased MDA levels and impaired antioxidant capacity have been reported[7]. In another study, co-exposure to $AlCl_3$ and acrylamide in rats induced oxidative stress, characterized by elevated MDA levels along with decreased GSH levels and reduced SOD and CAT activities[24].

In light of these findings, oxidative stress parameters were assessed in the $AlCl_3$-induced cardiotoxicity model. Consistent with previous reports, $AlCl_3$ exposure in the present study resulted in significantly elevated MDA levels together with marked reductions in GSH levels and SOD and CAT activities compared with the other experimental groups. These results suggest that $AlCl_3$ contributes to oxidative stress in cardiac tissue, at least in part, through impairment of the antioxidant defense system.

Inflammation and oxidative stress represent closely interconnected pathophysiological processes involving multiple mechanisms [12]. Elevated oxidative stress resulting from $AlCl_3$ exposure has been reported to contribute to the activation of inflammatory pathways, with both processes having a critical role in the progression of toxicity[22]. In a rat study, $AlCl_3$ administration was associated with a dose-dependent increase in pro-inflammatory cytokines, including TNF-α and IL-6 5. Likewise, experimental studies in mice have shown that $AlCl_3$ exposure activates inflammatory pathways in cardiac tissue, resulting in marked increases in pro-inflammatory cytokine levels, including IL-1β, IL-6, and TNF-α[25].

Accordingly, TNF-α and IL-1β levels in cardiac tissue were evaluated in the present study to assess the inflammatory response. Our findings demonstrated significantly higher TNF-α and IL-1β levels in the $AlCl_3$-treated rats than in the control groups. Collectively, these findings suggest that $AlCl_3$ promotes inflammatory responses by enhancing the production of pro-inflammatory cytokines, consistent with previous studies.

iNOS, a key component of inflammatory processes, is an important enzyme that mediates the interaction between oxidative stress and inflammation[26]. In a study evaluating the protective effects of cranberry extract and losartan against cardiomyopathy associated with $AlCl_3$-induced hepatorenal damage in rats, $AlCl_3$ exposure was reported to enhance the inflammatory response in cardiac tissue, accompanied by increased iNOS levels[23]. However, studies on iNOS in $AlCl_3$-induced cardiotoxicity are limited and largely biochemical; thus, our immunohistochemical assessment may offer complementary insight. Moreover, Al exposure has been reported to disrupt the structural integrity of cardiac tissue, resulting in necrosis, fibrotic changes, vascular alterations, and myocardial degeneration, with these effects being closely associated with mechanisms mediated by oxidative stress and inflammation[22,27]. The organization of collagen fibers within cardiac tissue plays a critical role in preserving myocardial contractile function and maintaining structural integrity[7]. In this context, α-SMA, a well-recognized marker of fibrotic activity, is considered to be associated with cardiac remodeling processes[9].

In the present study, immunohistochemical assessment of iNOS and α-SMA immunoreactivity, together with histopathological findings, indicated that $AlCl_3$ exposure induced inflammatory and profibrotic responses in heart tissue. Notably, $AlCl_3$ exposure resulted in evident tissue damage, including disruption of myocardial architecture, inflammatory cell infiltration, and vascular congestion. Although α-SMA immunoreactivity was markedly increased in the $AlCl_3$ group, the corresponding fibrotic alterations observed in Masson's trichrome-stained sections were relatively limited. This finding may suggest that profibrotic processes had been initiated at the molecular level but had not yet progressed sufficiently to produce overt histological fibrosis detectable by light microscopy.

Medicinal plants and their bioactive constituents have attracted increasing attention as potential therapeutic agents for the prevention and treatment of cardiotoxicity[12]. ESC, a naturally occurring coumarin derivative present in various medicinal plants, is

recognized for its potent antioxidant, anti-inflammatory, and antifibrotic properties[15,28,29]. In a study on the protective effect of ESC against doxorubicin-induced cardiotoxicity in Sprague-Dawley rats, intraperitoneal administration of ESC at doses of 50 and 100 mg/kg significantly reduced increased lipid peroxidation in the heart tissue; additionally, it was shown to significantly increase GSH levels, SOD, and CAT activities by restoring the decreased antioxidant activity[13]. In another study, ESC administration in an isoproterenol-induced myocardial injury model was reported to increase antioxidant enzymes (CAT, SOD, and GSH) while suppressing the inflammatory response (TNF-α and IL-6), thereby alleviating histopathological damage in cardiac tissue[29]. Additionally, in a cyclophosphamide-induced model of cardiac and renal injury, ESC administration was found to reduce lipid peroxidation, enhance GSH levels, and increase SOD and CAT activities. Moreover, it mitigated the inflammatory response by lowering IL-1β levels and consequently alleviated tissue damage[30].

Considering these biological activities of ESC, the present study evaluated the effects of two different doses of ESC (50 and 100 mg/kg) in an $AlCl_3$-induced cardiotoxicity model, focusing on oxidative stress, inflammation, histopathological alterations, and immunohistochemical changes. The findings showed that ESC treatment ($AlCl_3$ + ESC50 and $AlCl_3$ + ESC100) reduced MDA levels while increasing GSH levels and enhancing SOD and CAT activities compared to the $AlCl_3$ group, suggesting a partial restoration of the disrupted antioxidant balance in cardiac tissue. In addition, decreased TNF-α and IL-1β levels in the ESC-treated groups indicate a potential suppression of the inflammatory response. Histopathological analyses indicated that myocardial injury was less severe in the ESC-treated groups; a relative enhancement in myofibril organization was noted, accompanied by a reduction in inflammatory cell infiltration and vascular congestion. Immunohistochemical assessments indicated a reduction in iNOS and α-SMA positivity, suggesting that inflammation and profibrotic alterations may have been constrained. Moreover, protective effects were observed in both ESC-treated groups, with generally greater improvements observed in the $AlCl_3$ + ESC100 group. One limitation of the present study is that although biochemical, histopathological, and immunohistochemical evaluations were performed, functional cardiac assessments were not conducted. Therefore, the findings primarily reflect the effects of ESC on cardiac injury rather than direct functional cardiac outcomes. Another limitation of the present study is the lack of a separate $AlCl_3$ + DMSO control group. Although no significant differences were observed between the Control and Vehicle groups, the potential influence of DMSO on the observed effects in the treatment groups cannot be completely excluded. This limitation should therefore be considered when interpreting the findings of the present study.

CONCLUSION

ESC may provide protection against $AlCl_3$-induced cardiotoxicity through modulation of oxidative stress and inflammatory processes. This effect appears to be linked to an improved antioxidant status, as evidenced by decreased MDA levels, increased GSH levels, enhanced SOD and CAT activities, and reduced TNF-α and IL-1β levels. ESC treatment was further associated with attenuation of cardiac tissue damage, including preservation of myocardial architecture, along with reduced inflammatory cell infiltration and vascular congestion. The reduced immunoreactivity of iNOS and α-SMA may further indicate a decrease in inflammation-related and profibrotic alterations. The findings support the protective effects of ESC against $AlCl_3$-induced cardiotoxicity, with generally greater

improvements observed in the $AlCl_3$ + ESC100 group. However, further studies are needed to confirm the underlying mechanisms and therapeutic value of ESC.

Ethical Approval: All experimental methods involving live animals used in the current study were approved by the Karabük University Local Ethics Committee (Approval number: 2025 /11-38).

Conflict of Interest: No conflict of interest is reported by the authors.

Financial Disclosure: This work was supported by the Karabük University Scientific Research Fund [KBÜBAP-25-DS-191].

REFERENCES

1. Ghorbel I, Elwej A, Chaabane M, et al. Protective effect of selenium against aluminium chloride induced cardiotoxicity in rats. Pharm Biomed Res 2017; 3: 19-25.

2. Hawas AMM, Rashed LA, Mohamed MAEH. Evaluation of glucosamine effect against heart and brain damage induced by Y-radiation or aluminium chloride in female rats. Braz Arch Biol Technol 2020; 63: e20180687.

3. Radi RA, Kandeil MA, Mohammed ET, et al. Neuroprotective effects of Chlorella vulgaris loaded niosomes via SIRT1 activation in aluminum chloride-induced Alzheimer's model. Sci Rep 2025; 15: 40361.

4. Yavuz H, Şimşek H, Akaras N, et al. Protective role of catechin hydrate against aluminum chloride-induced nephrotoxicity via oxidative stress, NF-κB, Bax/Bcl-2, and PERK-CHOP pathways. Eur J Pharmacol 2025; 1008: 178341.

5. Anyiom OP, Samuel IF, Sunny K, et al. Cardiotoxicity induced by high doses of aluminium chloride. A histomorphological and biochemical study. TIJER-Int Res J 2026; 13.

6. Jackson JS, Rout P. Aluminum Toxicity. In: StatPearls [Internet]. Treasure Island (FL): StatPearls Publishing; 2024.

7. Jabeen K, Rehman K, Awan FR, et al. Comparative biochemical profiling of aluminum chloride and sodium azide induced neuroinflammation and cardiometabolic disturbance. ACS Omega 2022; 7: 40432-45.

8. Keçeci M, Bodur F, Babaoğlu E, et al. Comparison of Histomorphometric Characteristics of Heart and Aorta in Young Adult and Aged Rats. Med J West Black Sea 2024; 8: 244-56.

9. He Y, Ling S, Sun Y, et al. DNA methylation regulates α-smooth muscle actin expression during cardiac fibroblast differentiation. J Cell Physiol 2019; 234: 7174-85.

10. Tayo AB, Abubakar J, Gulumbe BH, et al. Cardio and neuroprotective effects of naringenin against aluminum chloride-induced oxidative stress in wistar rats. Avicenna J Med Biochem 2024; 12: 19-29.

11. Kundnani NR, Passini V, Stefania Carlogea I, et al. Overview of Oncology: Drug-induced cardiac toxicity. Medicina (Kaunas) 2025; 61: 709.

12. Leal LE, Moreira ES, Correia BL, et al. Comparative study of the antioxidant and anti-inflammatory effects of the natural coumarins 1,2-benzopyrone, umbelliferone and esculetin: in silico, in vitro and in vivo analyses. Naunyn Schmiedebergs Arch Pharmacol 2024; 397: 173-87.

13. Öztürk N, Karağaç MS, Yeşilkent EN, et al. Exploring esculetin's protective role: Countering doxorubicin-induced oxidative stress in rat heart. Lab Anim Sci Pract J 2024; 4: 44-52.

14. Kizir D, Yeşilkent EN, Öztürk N, et al. The protective effects of esculetin against doxorubicin-induced hepatotoxicity in rats: insights into the modulation of caspase, FOXOs, and heat shock protein pathways. J Biochem Mol Toxicol 2024; 38: e23861.

15. Demir Y, Ceylan H, Yeşilkent EN, et al. Esculetin attenuates doxorubicin-induced cardiac toxicity: Evidence from gene expression, enzyme activity, and molecular docking analyses. Comput Biol Chem 2026; 120: 108654.

16. Amini H, Karami M. Preliminary of cognitive and systemic disorders in rats due to chronic exposure to aluminum chloride. Caspian J Neurol Sci 2025; 11: 203-12.

17. Erdemli Z, Zayman E, Gokturk N, et al. The protective effects of thymoquinone against

tartrazine-induced pancreatic injury and its impact on oxidative stress, caspase 3, blood glucose, insulin and cholesterol levels. Arch Physiol Biochem 2026; 132: 1-11.

18. Alqhtani HA. Evaluation of L-carnitine's protective properties against AlCl3-induced brain, liver, and renal toxicity in rats. PLoS One 2025; 20: e0317939.

19. Ali FE, Badran KS, Baraka MA, et al. Mechanism and impact of heavy metal-aluminum (Al) toxicity on male reproduction: Therapeutic approaches with some phytochemicals. Life Sci 2024; 340: 122461.

20. El-Demerdash FM, Ahmed MM, Kang W, et al. Hepatoprotective effect of silymarin-chitosan nanocomposite against aluminum-induced oxidative stress, inflammation, and apoptosis. Tissue Cell 2024; 91: 102591.

21. Alasfar RH, Isaifan RJ. Aluminum environmental pollution: the silent killer. Environ Sci Pollut Res Int 2021; 28: 44587-97.

22. Tinkov AA, Skalny AV, Domingo JL, et al. A review of the epidemiological and laboratory evidence of the role of aluminum exposure in pathogenesis of cardiovascular diseases. Environ Res 2024; 242: 117740.

23. Galal SM, Hasan HF, Abdel-Rafei MK, et al. Synergistic effect of cranberry extract and losartan against aluminium chloride-induced hepatorenal damage associated cardiomyopathy in rats. Arch Physiol Biochem 2019; 125: 357-66.

24. Ghorbel I, Khemakhem M, Boudawara O, et al. Effects of dietary extra virgin olive oil and its fractions on antioxidant status and DNA damage in the heart of rats co-exposed to aluminum and acrylamide. Food Funct 2015; 6: 3098-108.

25. Cao C, Li X, Fu Q, et al. Selenium-rich-yeast protects against aluminum-induced activating nuclear xenobiotic receptors and triggering inflammation and cytochromes p450 systems in mice heart. Biol Trace Elem Res 2020; 194: 244-50.

26. Papi S, Ahmadizar F, Hasanvand A. The role of nitric oxide in inflammation and oxidative stress. Immunopathol Persa 2019; 5: e08.

27. El-Hussainy EHM, Hussein AM, Abdel-Aziz A, et al. Effects of aluminum oxide (Al2O3) nanoparticles on ECG, myocardial inflammatory cytokines, redox state, and connexin 43 and lipid profile in rats: possible cardioprotective effect of gallic acid. Can J Physiol Pharmacol 2016; 94: 868-78.

28. Chen J, Xia B, Zhou R, et al. Esculetin attenuates inflammation and fibrosis to prevent aki-to-ckd transition in adenine-induced renal injury by inhibiting the EGFR/SRC/PI3K/AKT/NF-κB signaling axis. Pharmaceuticals 2026; 19: 578.

29. Pullaiah CP, Nelson VK, Rayapu S, et al. Exploring cardioprotective potential of esculetin against isoproterenol-induced myocardial toxicity in rats: in vivo and in vitro evidence. BMC Pharmacol Toxicol 2021; 22: 43.

30. Srirangan P, Shyam M, Radhakrishnan V, et al. Therapeutic potential of esculetin in attenuating kidney and heart damage caused by cyclophosphamide: insights into NRF2 activation and NLRP3 inhibition. Mol Cell Toxicol 2026; 22: 289-308.